Article

Cell Reports

Retinal Proteoglycans Act as Cellular Receptors for Basement Membrane Assembly to Control Astrocyte Migration and Angiogenesis

Graphical Abstract

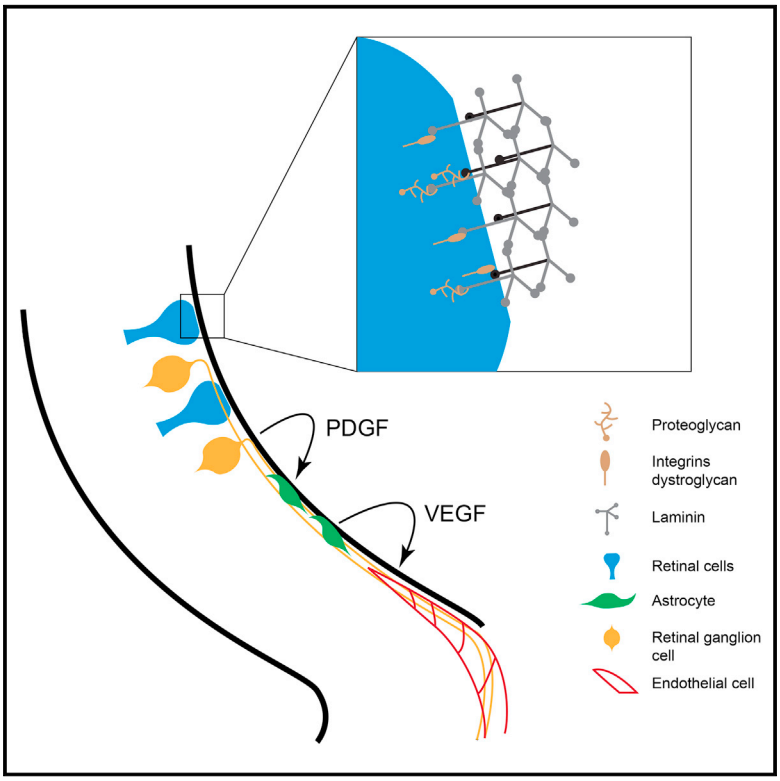

Authors

Chenqi Tao, Xin Zhang

Correspondence

xz2369@columbia.edu

In Brief

Neural-glial-endothelial interactions are vital for development and homeostasis of the nervous system. In the neural retina, Tao and Zhang suggest that cell-surface proteoglycans participate in the assembly of the basement membrane, which serves as an adhesive substrate for astrocyte migration.

Highlights

- Retinal proteoglycans are receptors for basement membrane assembly
- Retinal basement membrane is a necessary migration substrate for astrocytes
- Migration of astrocytes into neural retina is required for subsequent angiogenesis
- PDGF signals independently of proteoglycans to guide astrocyte migration

Tao & Zhang, 2016, Cell Reports *17*, 1832–1844
November 8, 2016
http://dx.doi.org/10.1016/j.celrep.2016.10.035

CellPress

OPEN ACCESS
CellPress

Cell Reports
Article

Retinal Proteoglycans Act as Cellular Receptors for Basement Membrane Assembly to Control Astrocyte Migration and Angiogenesis

Chenqi Tao[1] and Xin Zhang[1,2,*]
[1]Departments of Ophthalmology, Pathology and Cell Biology, Columbia University, New York, NY 10032, USA
[2]Lead Contact
*Correspondence: xz2369@columbia.edu
http://dx.doi.org/10.1016/j.celrep.2016.10.035

SUMMARY

The basement membrane is crucial for cell polarity, adhesion, and motility, but how it is assembled on the cell surface remains unclear. Here, we find that ablation of glycosaminoglycan (GAG) side chains of proteoglycans in the neuroretina disrupts the retinal basement membrane, leading to arrested astrocyte migration and reduced angiogenesis. Using genetic deletion and time-lapse imaging, we show that retinal astrocytes require neuronal-derived PDGF as a chemoattractive cue and the retinal basement membrane as a migratory substrate. Genetic ablation of heparan sulfates does not produce the same defects as GAG null mutants. In contrast, enzymatic removal of heparan sulfates and chondroitin sulfates together inhibits de novo laminin network assembly. These results indicate that both heparan and chondroitin sulfate proteoglycans participate in retinal basement membrane assembly, thus promoting astrocyte migration and angiogenesis.

INTRODUCTION

As the largest cell population in the CNS, astrocytes regulate numerous developmental and physiological events. In the eye, one of the earliest and most significant contributions of astrocytes is the control of retinal angiogenesis (Tao and Zhang, 2014). The simple observation that retinal astrocytes are absent in animals with avascular retinae such as birds, echidna, and horse indicates a close association of astrocytic and vascular networks (Schnitzer, 1987; Stone and Dreher, 1987). Examination of mouse retinae reveals that retinal vasculature invades the neonatal retina along preexistent scaffolds of astrocytes, which secrete angiogenic factors and extracellular matrix to promote migration of endothelial cells (Dorrell and Friedlander, 2006; Gerhardt et al., 2003; Hirota et al., 2011). This process is accompanied by progressive regression of hyaloid vessels, the primitive vasculature in the vitreous that nourishes the embryonic retinae and lens (Lang, 1997). Astrocytic malfunction can lead to impaired retinal vascularization, breakdown of the blood-retinal barrier, and reactive gliosis, contributing to a cohort of blinding diseases such as retinopathy of prematurity (ROP), coloboma, and glaucoma (Chu et al., 2001; Morgan, 2000; Stone et al., 1996; Volterra and Meldolesi, 2005).

Retinal astrocytes are born in the optic stalk and migrate from the optic nerve head to populate the retinal surface (Tao and Zhang, 2014). The temporal and spatial pattern of retinal ganglion cells (RGCs), astrocytes, and endothelial cells arising in the retina led to the classic sequential-induction model. It posits that RGC-derived platelet derived growth factor, alpha (PDGFA) attracts the invasion of astrocytes, which in turn, by providing a gradient of VEGFA, directs retinal angiogenesis. In support of this, inhibition of PDGFA signaling in the eye impaired the formation of astrocyte and vascular network (Fruttiger et al., 1996). However, knockout of *PDGFA* reduced the number of astrocytes but did not abolish their migration and occupation of the retina (Gerhardt et al., 2003). Transgenic overexpression of *PDGFA* increased the density of retinal astrocytes, but it retarded instead of accelerated the migration of astrocytes (Fruttiger et al., 1996). More recently, astrocyte-specific deletion of *VEGFA* failed to disrupt developmental angiogenesis of the retina, although hypoxia-induced neovascularization was impaired (Scott and Fruttiger, 2010; Weidemann et al., 2010). These experiments challenged the sequential-induction model in general and raised questions about the mechanism of astrocyte navigation in the retina.

Astrocyte migration also requires the basement membrane of the retina, termed the inner limiting membrane (ILM), as the traction substrate. Disruption of the ILM in laminin mutants leads to impaired astrocyte migration and retinal angiogenesis, but how the laminin network is established to form the ILM is not well understood (Gnanaguru et al., 2013; Pinzón-Duarte et al., 2010). Intraocular transplantation experiments have previously shown that mouse retina grafted into the chick eye can assembly a de novo ILM using the existing chick basement membrane components from the vitreous (Halfter et al., 2000). In contrast, no such basement membrane was formed when the dorsal root ganglion was transplanted. The remarkable difference in their ability to assemble basement membrane is thought to depend on the tissue-specific expression of cellular receptors, which recruit and promote the polymerization of laminins on the cell surface (Hohenester and Yurchenco, 2013). Previous studies have shown that integrins, dystroglycan, and sulfated glycolipids may act

as such receptors through their binding to the laminin G-like (LG) domains. However, genetic evidence indicates that none of these factors are universally required for basement membrane assembly (Yurchenco and Patton, 2009).

Proteoglycans are heavily glycosylated proteins with covalently linked glycosaminoglycan (GAG) side chains, which can be classified into five main categories: chondroitin sulfate (CS), heparin sulfate (HS)/heparin, dermatan sulfate (DS), keratin sulfate (KS), and hyaluronic acid (HA) (Esko and Selleck, 2002; Häcker et al., 2005). One of the rate-limiting enzymes in GAG synthesis is UDP-glucose 6-dehydrogenase (Ugdh), which produces UDP-α-d-glucuronic acid (UDP-GlcA), the donor substrate for a variety of transferases that incorporates the D-glucuronosyl moiety into the growing GAG chains. GAGs have binding affinity with a wide range of extracellular matrix (ECM) components and signaling molecules, allowing proteoglycans to actively regulate a variety of biological processes (Bishop et al., 2007). These include mediating cell adhesion in concert with integrin, serving as co-receptors for signaling molecules by facilitating ligand-receptor interaction, functioning as a repository for GAG-binding factors that can be liberated at a later stage by shedding, generating a morphogen gradient by sequestering the otherwise freely diffusible ligands to the cell surface. Indeed, both PDGFA and VEGFA possess alternatively spliced isoforms that contain binding motives for heparan sulfate proteoglycans (HSPGs) (Fruttiger et al., 1996; Ruhrberg et al., 2002; Stalmans et al., 2002). In this study, we genetically ablated the key GAG biosynthetic gene *Ugdh* in neural retina, demonstrating that proteoglycans are required non-cell-autonomously for astrocyte migration and angiogenesis. We showed that platelet derived growth factor (PDGF) is the chemoattractive cue for astrocytes, but it acts independently of proteoglycans. Instead, both HS and CS participate in the assembly of the retinal basement membrane, which serves as the migratory substrate for astrocytes. These results reveal the important role of neuroretinal-derived proteoglycans in regulating cell adhesion during astrocyte migration and retinal angiogenesis.

RESULTS

Proteoglycans Non-Cell-Autonomously Regulate Astrocyte Migration and Angiogenesis

In retinal development, astrocytes and endothelial cells spread from the central optic disc to the peripheral retina in a sequential manner. This migration pattern can be seen clearly in early postnatal retina, where Pax2-positive astrocytes have already reached the edge of the retina (Figures 1A and 1E, dotted line), followed by IB4-staining endothelial cells trailing behind. To investigate the role of proteoglycans in this process, we generated retinal-specific ablations of *Ugdh*, a key biosynthetic gene for GAGs. We first used *Six3-Cre*, a *Cre* deletor active in both the central retina (CR) and the optic stalk (OS) (Figures 1B and S1A) (Cai et al., 2013; Furuta et al., 2000), and we observed clear defects in astrocyte migration and angiogenesis. In *Six3-Cre; Ugdh*$^{flox/flox}$ retina, rudimentary sprouts of blood vessels were confined to the central retina and astrocytes congregated around the optic disc (OD), apparently unable to migrate into the peripheral retina (Figure 1F). Since *Six3-Cre* targeted both the neural retina and astrocytes that spread from the optic stalk to the superficial layer (SL) of the retina, we next used *GFAP-Cre* to disrupt proteoglycans specifically in astrocytes (Figures 1C and S1B) (Zhuo et al., 2001). Interestingly, there was no obvious phenotype in *GFAP-Cre; Ugdh*$^{flox/flox}$ retina (Figure 1G), suggesting that GAGs were not required within astrocytes for their migratory behavior. To further confirm this finding, we took advantage of another Cre deletor, *α-Cre*, which was restricted to the peripheral neural retina (PR) (Figures 1D and S1C) (Cai et al., 2011; Marquardt et al., 2001). Although *α-Cre* was not active in astrocytes, we again observed that astrocytes failed to invade the peripheral retina, which were instead associated with residual hyaloid vessels (Figures 1H and S2A). Taken together, these results showed that neuroretinal-derived proteoglycans were non-cell-autonomously required for migration of astrocytes and endothelial cells.

To understand the cause of astrocyte migration and angiogenesis defects, we focused on *α-Cre; Ugdh*$^{flox/flox}$ mutants, which lost GAGs only in the neural retina. As astrocytes were sweeping toward the peripheral retina, a bromodeoxyuridine (BrdU) labeling experiment failed to detect any obvious changes in their proliferation rate (Figures 1I–1K). The proliferation and migration of retinal endothelial cells are driven at least in part by VEGFA secreted by astrocytes in front of the vascular plexus, and these astrocytes sharply downregulate *Vegfa* expression after the passing of the endothelial wave front (Figures 1L and 1N, arrowheads). Consistent with a lack of astrocytes in the peripheral retina, *Ugdh* mutants were devoid of *Vegfa* ahead of the endothelial cells in the superficial layer of the retina (Figure 1M, asterisk), despite a compensatory increase of *Vegfa* in the deep layer (Figure 1O, arrow). Considering the critical role of astrocytes in retinal angiogenesis, we concluded that the vasculature defects is secondary to the failure of astrocyte migration.

Proteoglycan Deficiency Causes Retinal Degeneration without Affecting Cell Differentiation

To exclude the possibility that impaired astrocyte migration in *Ugdh* mutants was caused by a retinal differentiation defect, we examined the major retina cell types. Retinal neurogenesis in mammals begins with retinal ganglion, amacrine, and horizontal cells born embryonically, followed by the later appearance of rod photoreceptors and bipolar and Müller cells. At postnatal day 3 (P3) when astrocyte migration defect first became visible, *α-Cre; Ugdh*$^{flox/flox}$ retinae appeared morphologically identical to wild-type controls (data not shown). Using Brn3a as marker for retinal ganglion cells, Pax6 for amacrine cells, Chx10 for bipolar cells, NF165 for horizontal cells, rhodopsin for photoreceptors, Sox2 for Müller glia, and β3-tubulin for retinal nerve fibers, we did not detect any cell differentiation defects (Figures 2A and S2B). By P10, when the birth of retinal neurons was complete, the number of each retinal cell type remained similar to those of wild-type controls, except that GFAP-positive astrocytes were missing from the superficial layer in the distal retina (Figure 2A, arrows). However, there were circular clusters of cells, also known as rosettes, that formed in the photoreceptor cell layer throughout the peripheral retina (Figure 2A, arrowheads), whereas the central retina was unaffected, which is consistent with the *α-Cre* excision pattern. Since rosette formation is a

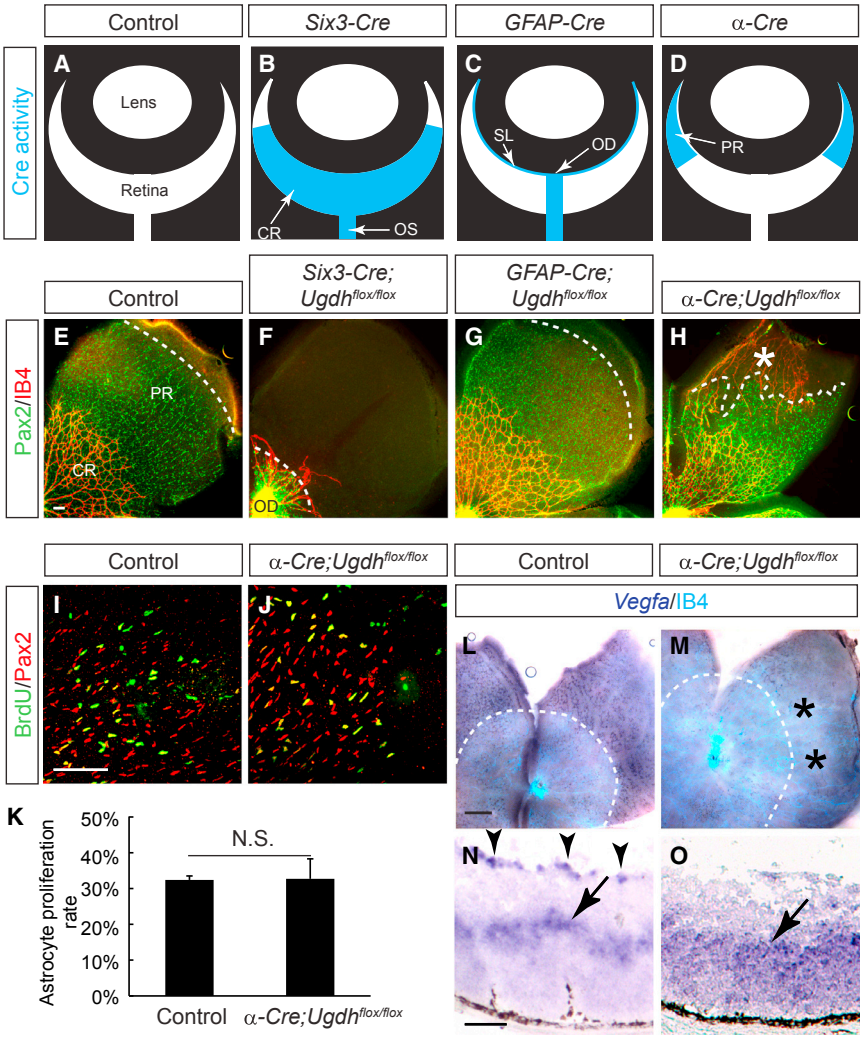

Figure 1. Tissue-Specific Requirement for Proteoglycans in Astrocyte Migration

(A–D) Schematic diagram of Cre activity. *Six3-Cre* is expressed in the central retina (CR) as well as the optic stalk (OS), *GFAP-Cre* in astrocytes that populate the optic stalk, the optic disc (OD), and the superficial layer (SL) of the retina, and α-*Cre* is expressed in the peripheral neuroretina (PR), but not in astrocytes.

(E–H) Ablation of proteoglycans in the central retina and the optic stalk by *Six3-Cre*-mediated deletion of *Ugdh* severely impaired astrocyte and vasculature development at postnatal day 3 (P3) (F). The disruption of astrocyte migration was also observed in retinal-specific knockout using α-*Cre* (H), but not in astrocyte-specific knockout using *GFAP-Cre* (G). Astrocytes were labeled by Pax2 and endothelial cells by IB4. Dashed curves represent the front of the astrocyte spread, and asterisks show persistent hyaloid vessels.

(I–K) BrdU labeling in *Ugdh* mutants indicated that proliferation was normal in astrocytes. The error bars in (K) represent SEM.

(L–O) *Vegfa* expression was upregulated in the astrocytes (arrowheads in N beyond the vasculature front [dashed curve in L in wild-type retina]), but it was lost in hyaloid-vessel-occupied area in α-*Cre; Ugdh*$^{flox/flox}$ retina (asterisks in M). Note that *Ugdh* mutant retina displayed an increase of VEGF expression in the inner nuclear layer (arrow in O). Scale bars, 100 μm.

hallmark of retinal degeneration, we next examined cell death by TUNEL staining. Physiological cell death occurs in retina during the first week after birth, but it should have ceased by P14. In contrast, extensive cell death was still detectable in P14 mutant retinae (Figure 2B). As a result, the peripheral retinae in 3-month-old *Ugdh* mutants were severely hypoplastic, with massive cell loss (Figure 2C). Therefore, proteoglycan deficiency resulted in extensive retinal degeneration.

We have previously shown that ablation of HS *N*-sulfotransferase genes (*Ndst1* and *Ndst2*) disrupts fibroblast growth factor (FGF) signaling, leading to optic stalk dystrophy and retinal degeneration (Cai et al., 2014). These phenotypes could be partially rescued by constitutive activation of downstream Ras-mitogen-activated protein kinase (MAPK) signaling. In *Ugdh* mutants, however, we did not detect any apparent loss of FGF signaling by phospho-extracellular signal-regulated kinase (ERK) staining (data not shown). Furthermore, using an inducible allele of oncogenic *Kras* (*Kras*^{G12D}), we showed that constitutively active Ras signaling was unable to ameliorate astrocyte migration defects in α-*Cre; Ugdh*$^{flox/flox}$*; LSL-Kras*^{G12D} retinae (Figures 3A–3C, asterisks). The stalled astrocytes in both mutants displayed significant increase in GFAP staining at P8 (Figures 3D and 3E, arrows), which was also visible in the cell body and the endfeet of Müller glia by P24 (Figures 3G–3I, arrow and arrowheads, respectively). The elevation of GFAP expression in astrocytes and Müller cells indicated massive gliosis, which likely contributed to retinal degeneration in adult animals.

PDGF Signaling Acts Independently of Proteoglycans to Direct Astrocyte Migration

The results above showed that retinal angiogenesis and degeneration defects in *Ugdh* mutants were preceded by astrocyte migration failure. This could be due to defective PDGF signaling, which has been implicated in astrocyte development (Fruttiger et al., 1996). Previous studies showed that injection of PDGFRα neutralizing antibody or knockout of *PDGFA* perturbed astrocyte patterning in retina, but an extensive astrocytic network still remained (Fruttiger et al., 1996; Gerhardt et al., 2003). To confirm the role of PDGF signaling in astrocyte migration, we used astrocyte-specific *GFAP-Cre* to ablate *PDGFRα*. Whole-mount immunostaining showed that P3 wild-type control retina was fully covered by an astrocytic network, but only a few scattered astrocytes appeared in the center of *GFAP-Cre; PDGFRα*$^{flox/flox}$ retina (Figure 4A). Close inspection of *PDGFRα* mutants revealed a few rudimentary vascular

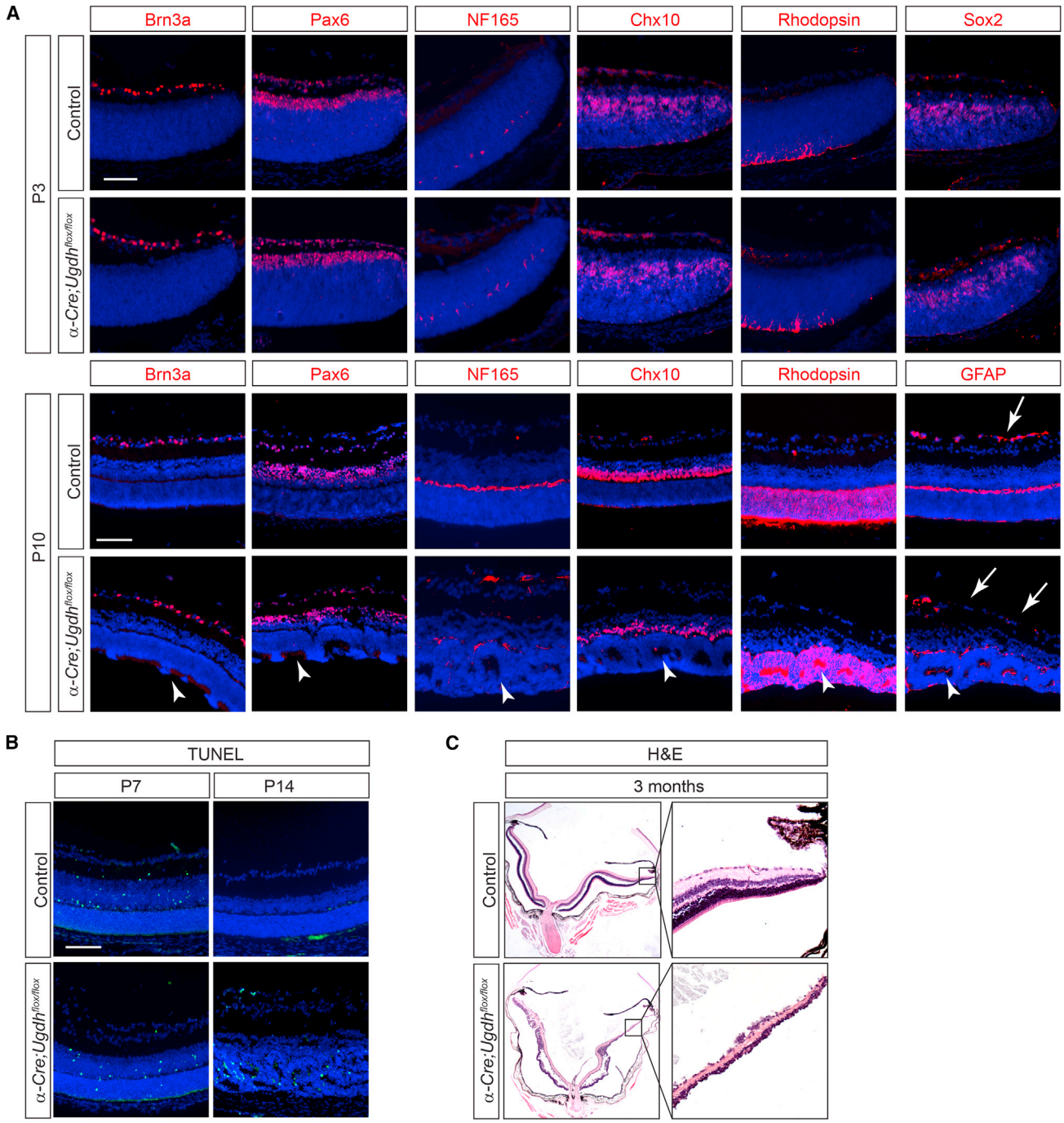

Figure 2. The *Ugdh* Mutant Retina Degenerates after Completing Normal Differentiation

(A) The major cell types in the retina, as indicated by Brn3a for retinal ganglion cells, Pax6 for amacrine cells, NF 165 for horizontal cells, Chx10 for bipolar cells, rhodopsin for rod photoreceptors, and Sox2 for Müller glia, emerged normally at P3 and P10. Note the lack of GFAP-positive astrocytes (arrows) and formation of rosettes (arrowheads) in mutant retina at P10.

(B) TUNEL staining indicated persistent apoptosis in *Ugdh* mutant retinae at P14.

(C) H&E staining of adult *Ugdh* mutant retinae showed severe degeneration at 3 months of age.

Scale bars, 100 μm.

sprouts, which aligned precisely with isolated groups of astrocytes (Figure 4A, enlarged images on the right). This is consistent with the idea that retinal astrocytes provide the critical guidance cue for endothelial cells, further supporting that the angiogenesis failure in *Ugdh* retina is caused by astrocyte patterning defect.

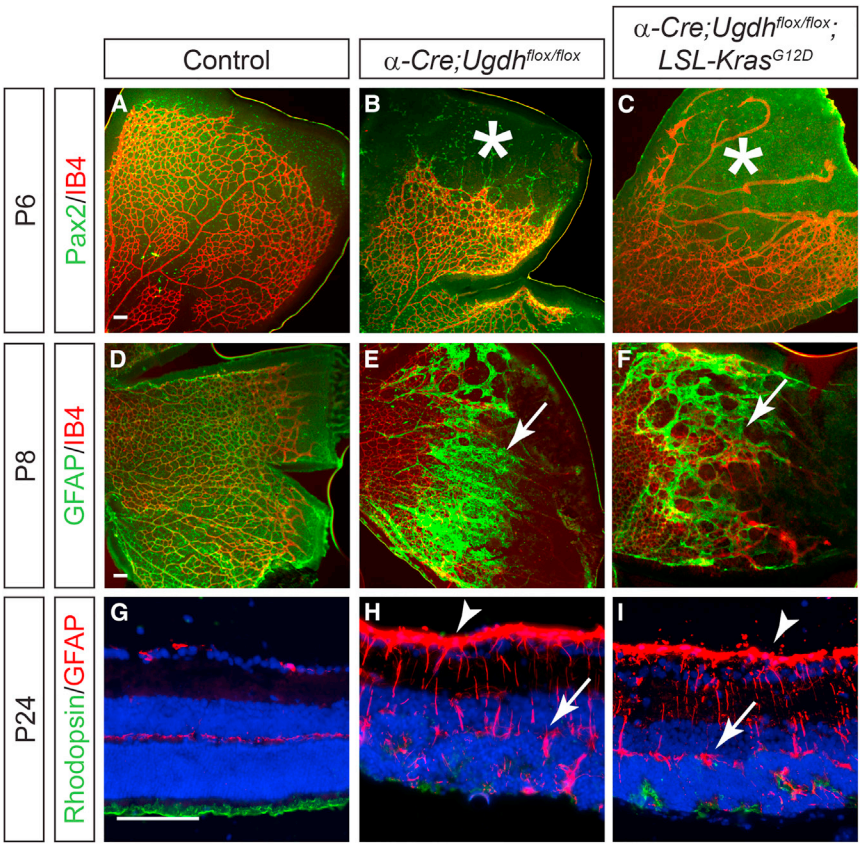

Figure 3. Constitutive Activation of Ras Signaling Fails to Rescue Astrocyte Migration Defects in the Ugdh Mutant

(A–C) α-Cre; Ugdh$^{flox/flox}$; LSL-Kras^{G12D} retinae exhibited the same defects in astrocyte migration, retinal angiogenesis, and hyaloid vessel persistence as α-Cre; Ugdh$^{flox/flox}$ mutants. Asterisks show persistent hyaloid vessels.

(D–I) Activation of Ras in α-Cre; Ugdh$^{flox/flox}$; LSL-Kras^{G12D} retina did not ameliorate reactive gliosis indicated by GFAP upregulation (arrows) and rosette formation in the photoreceptor layer (arrowheads).

Scale bars, 100 μm.

Proteoglycans may serve as co-receptors for PDGF in signal recipient cells (Rolny et al., 2002), but we consider this mechanism unlikely in the context of astrocyte migration, because astrocyte-specific ablation of GAGs in *GFAP-Cre; Ugdh$^{flox/flox}$* retina failed to produce any phenotype (Figure 1G). Another potential mechanism we considered is that proteoglycans bind directly to PDGFA, converting it from a freely diffusible chemoattractant to a substrate-bound haptotactic signal. Murine PDGFA can be expressed in two isoforms as a result of alternative splicing of exon 6, which encodes a cell-retention motif that confers binding to extracellular matrix molecules, including HSPGs (Abramsson et al., 2007; Feyzi et al., 1997; Smith et al., 2009). However, by qPCR using primers targeting exons 4 and 5, we showed that the total PDGFA (PDGFA$_T$) was expressed in both kidney and retina (Figure 4B). In contrast, the "long" isoform of PDGFA (PDGFA$_L$) detectable by primers against exon 6 was only present in kidney. Furthermore, the total amount of PDGFA (PDGFA$_T$) was similar between wild-type and *Ugdh* mutant retinae.

Finally, we established an ex vivo astrocyte migration assay to examine the functional requirement of PDGF isoforms. It took advantage of a *PDGFRα^{GFP}* knockin allele that expresses GFP specifically in astrocytes (Hamilton et al., 2003). Neonatal *PDGFRα$^{GFP/+}$* retina removed of the lens and the retinal pigmented epithelium was placed on a transparent filter. After insertion of PDGF-soaked beads at the peripheral retina, the explant was incubated over culture medium, and the GFP-expressing astrocytes were monitored by an inverted microscope (Figure 4C). Time-lapse imaging showed that astrocytes migrated toward the PDGF beads over 48 hr, eventually forming a dense halo around the beads (Figure 4D). As control, fibroblast growth factor (FGF)-, epidermal growth factor (EGF)-, or BSA-soaked beads failed to affect astrocyte migration (Figure 4E; data not shown). Although PDGFA$_S$ did not have the proteoglycan binding motif, it was equally efficient as PDGFA$_L$ in attracting astrocytes (Figure 4E; quantification shown in Figure 7F). Taken together, these experiments demonstrate that PDGF is necessary and sufficient to promote astrocyte migration in retina, but it does not require interaction with proteoglycans to function as a chemoattractant.

The Basement Membrane of the Retina Is Disrupted in the Proteoglycan Mutant

Directed cell migration requires not only directional cues but also appropriate migratory substrates. Having ruled out the role of proteoglycans in PDGF-induced chemotaxis, we next turned to its potential involvement in cell adhesion. Given that our genetic analysis suggests that GAG functions non-cell-autonomously in astrocyte migration, we asked whether neuronal-derived proteoglycans may indirectly regulate the extracellular matrix that interacts with astrocytes. The commonly used heparan sulfate antibody 10E4 stained many tissues, including the lens, but it reacted poorly with the retina (data not shown). We instead performed ligand and carbohydrate engagement assay (LACE) by incubating tissue sections with Fgf10 and Fgfr2/immunoglobulin G (IgG) fusion protein, followed by secondary antibody against the IgG domain. Because of the high-affinity binding of Fgf10/Fgfr2 with HS, this method has been shown to detect endogenous heparan sulfates with high sensitivity (Allen and Rapraeger, 2003; Pan et al., 2008). At embryonic day 13 (E13), both wild-type and *α-Cre; Ugdh$^{flox/flox}$* mutants displayed ubiquitous LACE staining throughout retinae (Figure 5A). Mosaic loss of LACE staining began to appear in mutant retina by E16, eventually widening to encompass the entire distal retina at birth (Figure 5A, arrows). Despite a complete absence of LACE staining in the

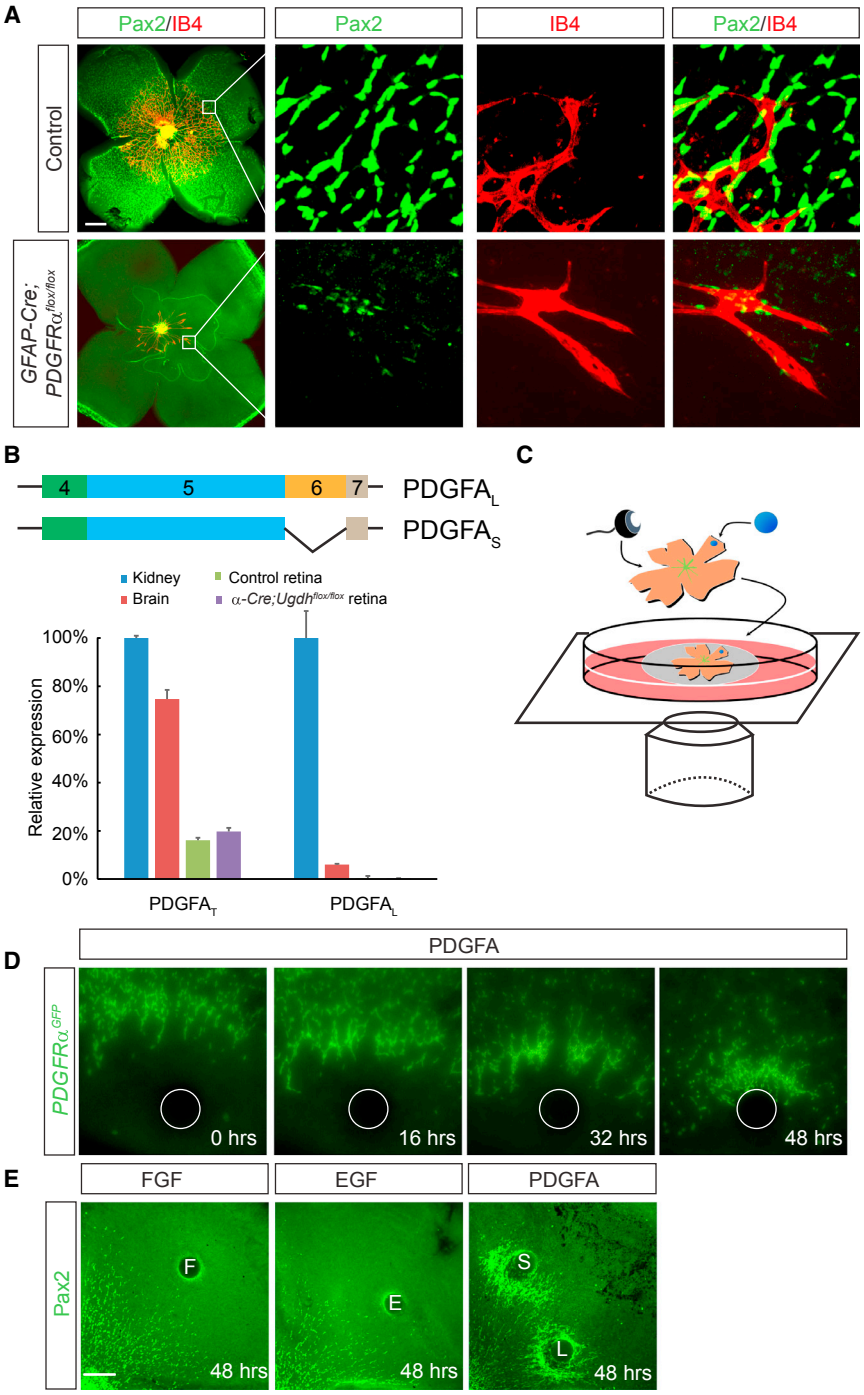

Figure 4. PDGF Induces Astrocyte Migration Independently of Retinal Proteoglycans

(A) Ablation of PDGFRα in astrocytes severely impaired astrocyte patterning and subsequent retinal angiogenesis. The boxes in the first column of images were enlarged and shown on the right. Note the close association between IB4-positive endothelial cells and a few escaped Pax2-positive astrocytes.

(B) An illustration of the long and short isoforms of PDGFA. qRT-PCR demonstrated that the retina only expressed $PDGF_S$, which lacks the proteoglycan-interaction motif encoded by exon 6. $PDGFA_L$, "long" isoform; $PDGFA_S$, "short" isoform; $PDGFA_T$, sum of the long and short isoforms. The error bars represent SEM.

(C) A diagram of the retina whole-mount culture with Affi-gel beads.

(D) Representative images from time-lapse imaging showing astrocytes labeled by *PDGFRα*^{GFP} that migrated toward PDGFA-coated beads over 48 hr.

(E) Both $PDGFA_S$ (S) and $PDGFA_L$ (L) beads were equally efficient in attracting astrocyte migration. Scale bars, 200 μm.

deep layers of mutant retina, a strong LACE signal remained in the superficial layer, which is the basement membrane of the retina, also known as the ILM (Figure 5A, arrowheads). Nevertheless, there were gaps in the LACE staining, suggesting that the ILM may be impaired in *Ugdh* mutants.

The persistent LACE staining in the ILM suggested that at least the majority of HSPGs within the ILM were produced outside the retina, because proteoglycans secreted by the underlying mutant retina would have lost the HS chain and LACE signal. This is consistent with previous studies in chick, which indicated that many of the basement membrane components were synthesized in the lens and ciliary body before being deposited onto the neuroretina to form the ILM (Halfter et al., 2005, 2008). To confirm this observation in mouse, we performed RNA in situ hybridization of *Perlecan*, the main HSPG of the basement membrane. Whereas *Perlecan* sense probe did not detect any signal, the antisense probe showed that *Perlecan* RNA was expressed exclusively in the lens (Figure 5B, arrow; data not shown). In contrast, immunostaining demonstrated that perlecan protein was present in both the lens capsule and the ILM (Figure 5B, arrowheads). Similar to LACE staining, perlecan expression in wild-type control appeared as a continuous smooth line over the retina, but *Ugdh* mutants displayed conspicuous gaps (Figure 5B, asterisks). This result further supported that there were significant breaches in the basement membrane of the retina.

To determine the extent of ILM defects, we next examined laminins and collagen IV, two major constituents of the basement membrane. Whole-mount immunostaining using a pan-laminin antibody revealed a smooth sheet of laminin network in wild-type retina, but the distal retina in *α-Cre; Ugdh*$^{flox/flox}$ mutants displayed many large holes, which were usually associated

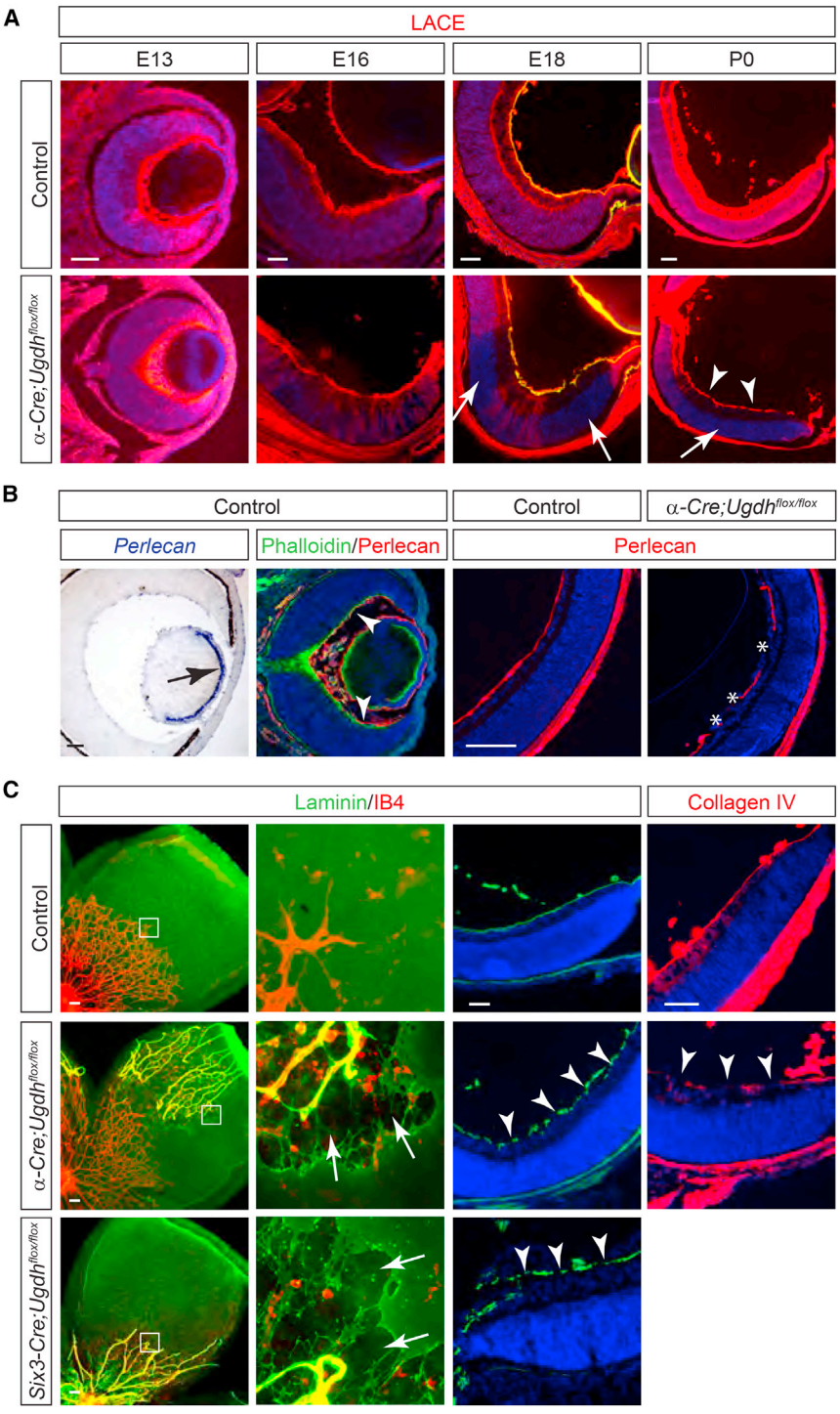

Figure 5. The Inner Limiting Membrane Is Disrupted in Proteoglycan-Deficient Retina

(A) Heparan sulfates were ablated in the deep layers of *Ugdh* mutant retina indicated by LACE staining (arrows). Note the persistent heparan sulfates in the inner limiting membrane on the superficial layer of the retina (arrowheads).

(B) Despite abundant perlecan protein in wild-type ILM (arrowhead), *perlecan* mRNA was produced by the lens (arrow), but not by the retina. The mutant ILM showed gaps in perlecan protein staining (asterisks).

(C) The laminin-stained ILM was smooth and continuous in wild-type retina but ruptured in both *α-Cre; Ugdh*$^{flox/flox}$ and *Six3-Cre; Ugdh*$^{flox/flox}$ mutants (arrows). Section staining with laminin and collagen IV antibodies also revealed a discontinuous ILM in *Ugdh* mutant (arrowheads).

Scale bar, 100 μm.

with persistent hyaloid vessels (Figure 5C, arrows). We also performed laminin staining in *Six3-Cre; Ugdh*$^{flox/flox}$ mutants, which lacked proteoglycans in the central retina. We observed extensive disruption of the laminin sheet surrounding the stalled endothelial cells. The disruption of the ILM was further confirmed by immunostaining of retinal sections, which showed significant gaps in both laminin and collagen IV networks (Figure 5C, arrowheads). Taken together, these results showed that loss of neuronal-derived proteoglycans disrupted the basement membrane of the retina.

Neuronal-Derived Proteoglycans Participate in the Assembly of the Retinal ILM

Secreted proteoglycans such as perlecan serve as cross linkers within the basement membrane (Costell et al., 1999). However, since we showed that perlecan was expressed exclusively by the lens, retinal-specific knockout of *Ugdh* was not expected to affect the biosynthesis and glycosylation of perlecan. This was also supported by our LACE experiment, which showed that HSPGs were still present in the remaining ILM overlying *Ugdh* mutant retina. To further examine the role of proteoglycans within the ILM, we performed enzymatic treatment of neonatal retinae (Figure S3A). Removal of HS or CS by heparinase or chondroitinase ABC (ChABC), respectively, did not impair the integrity of the ILM, as judged by pan-laminin staining (Figures S3B–S3D). In agreement with previous reports, collagenase digestion abrogated the retinal ILM (Figure S3E). These results suggested that glycosylation of proteoglycans within the ILM was not essential for the maintenance of this retinal basement membrane.

We next focused on proteoglycans tethered to the retinal cell surface and asked whether the GAG side chains of these membrane-bound proteins were involved in the assembly of the ILM.

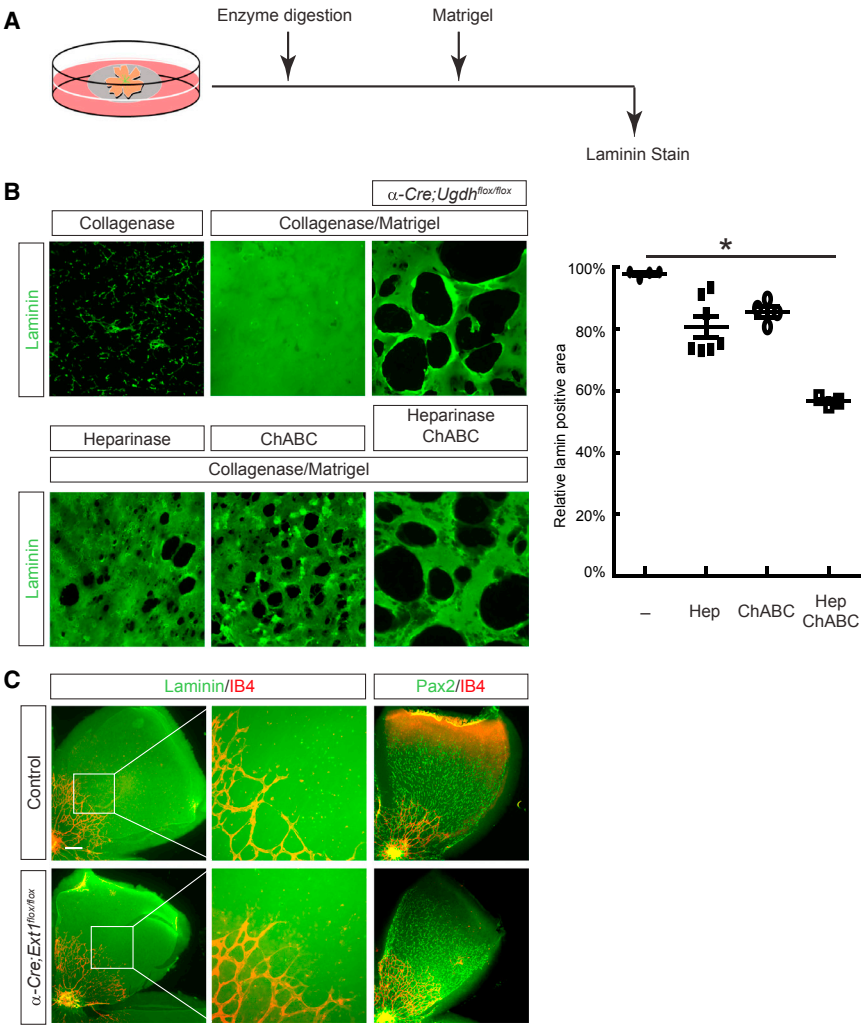

Figure 6. ILM Assembly Requires Retinal Heparan Sulfates and Chondroitin Sulfates

(A) A schematic diagram of the ILM reconstitution assay. After enzymatic digestion to remove the endogenous ILM, the retina was incubated in Matrigel supplemented with laminin to assemble a new laminin network.

(B) Collagenase treatment stripped the ILM off the retina, but the laminin sheet could be reconstituted after Matrigel incubation. In contrast, reconstitution was poor in the α-*Cre; Ugdh*$^{flox/flox}$ mutant, which displayed many large holes in laminin staining. When collagenase-treated retina was also digested with heparinase I and III or ChABC to remove heparan sulfates and chondroitin sulfates, respectively, the laminin sheet was partially recovered by Matrigel incubation. Combined digestion of heparinase I and III and ChABC further disrupted laminin reconstitution on wild-type retina to an extent comparable to the fragmented laminin network on the α-*Cre; Ugdh*$^{flox/flox}$ mutant. The relative coverage of retina by laminin staining is quantified on the right. The error bars represent SEM. *$p < 0.05$.

(C) Ablation of heparan sulfates alone failed to disrupt the laminin-staining ILM in the α-*Cre; Ext1*$^{flox/flox}$ mutant. Both astrocyte migration and angiogenesis proceeded without interruption. Scale bar, 200 μm.

In experiments depicted in Figure 6A, neonatal retinae were first stripped off ILM by collagenase treatment, followed by incubation in Matrigel supplemented with laminins. After this Matrigel reconstitution experiment, immunostaining revealed a smooth sheet of laminins on top of wild-type retina (Figure 6B). In contrast, *Ugdh* mutants still showed fragmented laminin staining, reminiscent of the fragmented ILM pattern in vivo. This suggested that *Ugdh*-deficient retina have an intrinsically defective ability to assemble a laminin network. Since Ugdh enzyme participates in the biosynthesis of both HS and CS, we next sought to identify which GAG chain was required for laminin assembly by the retina. Interestingly, digestion of wild-type retina with either heparinase or ChABC only partially disrupted the reconstitution of laminin network in our assay. Combined treatment of both heparinase and ChABC, however, resulted in numerous large holes in laminin staining, similar to what was observed in *Ugdh* mutant retina. Altogether, these data suggest that retinal GAGs are important for the assembly of the laminin matrix.

The synergistic effect of HS and CS removal in our Matrigel reconstitution assay suggested that these two GAGs may compensate for each other during ILM assembly. To test this hypothesis, we genetically ablated Ext1, the HS polymerase essential for the initial synthesis of all HS chains. In α-*Cre; Ext1*$^{flox/flox}$ retina, there was no breach in the ILM as shown by laminin staining (Figure 6C). As a result, astrocytes still migrated to the periphery of the retina, and the formation of retinal vasculature was unperturbed. The lack of ILM and astrocyte defects in *Ext1* mutant retina was in stark contrast to the *Ugdh* mutant generated using the same α-*Cre* deletor. This leads us to conclude that HS and CS play redundant roles in ILM assembly.

PDGF-Induced Astrocyte Migration Requires an Intact ILM

Previous studies have shown that laminin mutations disrupted the formation of an astrocytic network (Edwards et al., 2010; Gnanaguru et al., 2013). This suggests that astrocyte migration failure in our proteoglycan mutants may be due to breaches in the ILM. According to this model, retinal astrocytes can sense the chemoattractive PDGF signal produced by retinal ganglion cells, but they are unable to migrate into the proteoglycan-deficient region because of the lack of the intact ILM as substrate (Figure 7A). This further predicts that astrocytes will unimpededly traverse wild-type retina in response to exogenous PDGF, but these cells will stall upon encountering proteoglycan-deficient retina. To test this idea, we performed the ex vivo astrocyte migration assay on α-*Cre; Ugdh*$^{flox/flox}$ retinae, followed by LACE staining to mark the boundary of proteoglycan ablation. When PDGFA

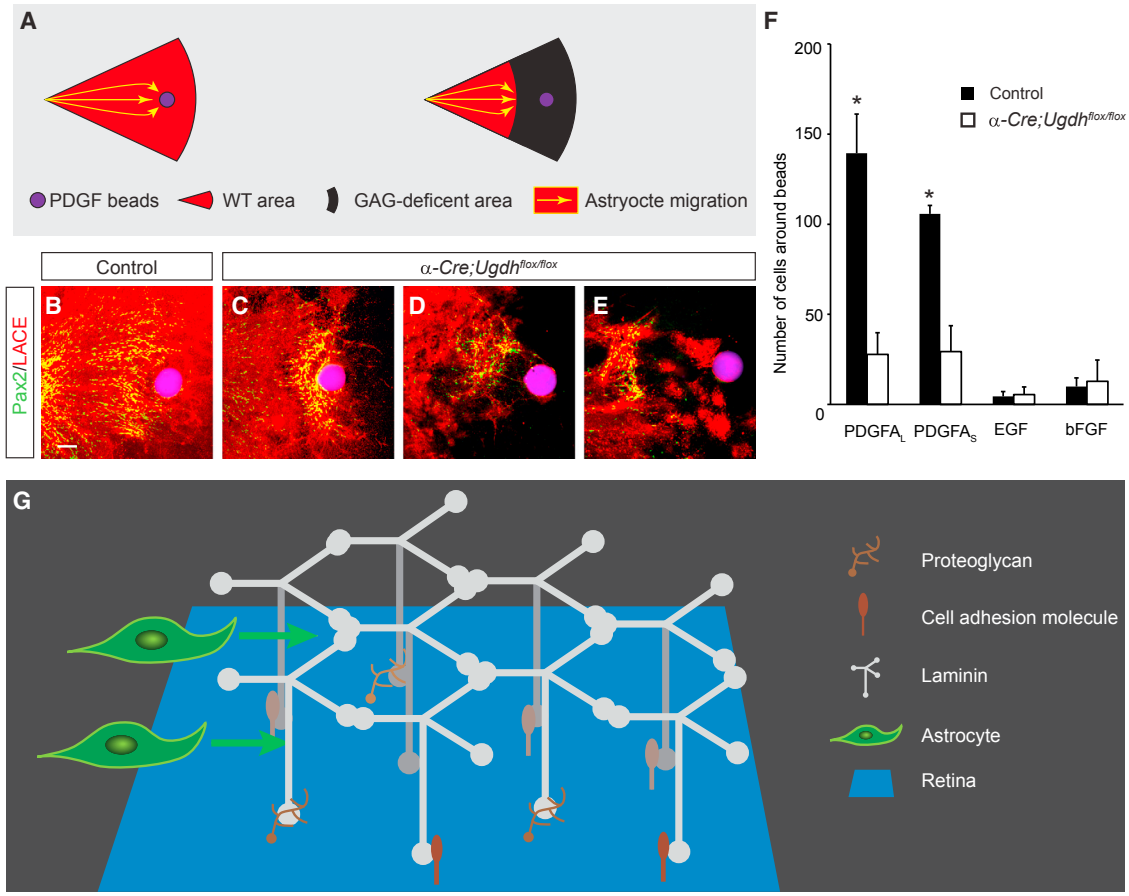

Figure 7. The ILM Defect in Proteoglycan-Deficient Retina Prevents PDGF-Induced Astrocyte Migration

(A–E) Astrocytes were attracted to PDGF-coated beads placed in wild-type retina. In the α-*Cre; Ugdh*$^{flox/flox}$ mutant, astrocytes were restricted to move in the wild-type area marked by LACE staining and were unable to reach the PDGF beads inside the proteoglycan-deficient area. This resulted in an accumulation of astrocytes on the border of the wild-type area.

(F) Quantification of astrocyte migration after exposure to different growth factors in both wild-type and *Ugdh* mutants. The error bars represent SEM. *$p < 0.01$.

(G) A model of cell-surface proteoglycans regulating the ILM assembly and astrocyte migration. Retinal-derived proteoglycans collaborate with other cell-adhesion molecules to bind laminins to the surface of the retina, promoting laminin polymerization and ILM assembly. Astrocytes use the ILM as an adhesive substrate to migrate into the retina.

Scale bar, 100 μm.

beads were placed at the edge of the mutant area, astrocytes migrated toward the beads as efficiently as those observed in wild-type control (Figures 7B and 7C). As PDGFA beads were moved further away and into the mutant region, however, astrocytes remained accumulated at the boundary of wild-type retina, apparently unable to move further (Figures 7D–7F). The astrocyte exclusion zone coincided with the breach of the ILM in the mutant area, supporting our model that proteoglycan-mediated assembly of the ILM is essential for astrocyte migration.

DISCUSSION

In this study, we show that retinal-derived proteoglycans potentiate the migration of astrocytes, which in turn recruit endothelial cells into the retina. This neural-glial-endothelial interaction is vital to ensure complete coverage of the retina by astrocytic and vascular networks. Our results further demonstrate that PDGF is the chemoattractive signal for astrocyte migration, but proteoglycan deficiency does not affect the production, propagation, or detection of PDGF. Instead, proteoglycans are directly involved in the assembly of the ILM, the retinal basement membrane that serves as migratory substrate for astrocytes (Figure 7G). The formation of the basement membrane is initiated by polymerization of laminins, which need to be anchored to cell-adhesion molecules. Our results identify cell-surface proteoglycans, including HS and CS, as cellular receptors in this process to promote the assembly and stability of the basement membrane.

In the sequential-induction model, retinal astrocytes respond to PDGF from retinal ganglion cells and secret vascular endothelial growth factor (VEGF) for endothelial cells, acting as a crucial link in the neural-glial-endothelial interaction. Recent studies, however, have raised questions regarding this paradigm. In mouse models that ablated Brn3a-positive retinal ganglion cells or inactivated their key developmental gene Math5, the

astrocytic network was still found in the retina (Edwards et al., 2012; Sapieha et al., 2008). The caveat for these studies, however, is that residual retinal ganglion cells likely existed in both mouse models. On the other hand, loss of VEGF production from astrocytes did not prevent retinal vasculature formation, casting doubt on the necessity of astrocyte-derived VEGF in retinal angiogenesis (Scott et al., 2010; Weidemann et al., 2010). Here, we showed that astrocyte-specific deletion of PDGFRα resulted in arrest of astrocyte migration, which further prevented retinal angiogenesis. This result was also consistent with previous reports that genetic ablation of HIF-2α or Tlx in astrocytes abolished retinal vasculature (Duan et al., 2014; Uemura et al., 2006), suggesting that the astrocytic network is indeed indispensable for retinal angiogenesis. Taken together, these observations suggest that astrocytes must also play additional roles in endothelial cell migration other than secreting VEGF. Astrocytes are known to secret fibronectin and HSPGs, both of which have been shown to regulate angiogenesis by sequestering VEGF. However, even combined ablation of fibronectin and HSPGs in astrocytes failed to reproduce the severity of the HIF-2α or Tlx knockout phenotype (Stenzel et al., 2011). It is notable that our *PDGFR*α mutant had a few stray astrocytes in the retina, likely because of an incomplete genetic inactivation. These escaped astrocytes were inevitably covered by endothelial cells, indicating that the close contact with astrocytes may be important for endothelial cells to invade the retina. Just as our results show that the neuroretina assembles the ILM to pave the path for astrocyte, astrocytes may also be needed to remodel the ECM to facilitate migration of endothelial cells.

Although PDGF signaling was implicated in astrocyte migration two decades ago, the nature of PDGF's requirement has not been resolved. PDGF can function as either a mitogen or a chemoattractant (Forsberg-Nilsson et al., 1998; Kang et al., 2008). In fact, a previous study showed that overexpression of PDGFA in retina promoted proliferation of astrocytes but retarded their migration (Fruttiger et al., 1996). It should be cautioned, however, that ubiquitous expression of PDGF at a high level may overwhelm any directional cue in the retina, confounding the interpretation of these results. By developing an ex vivo model of astrocyte migration, we were able to use time-lapse imaging to show that astrocytes indeed migrate toward PDGF-containing beads, suggesting astrocytes can sense a chemoattractive gradient of PDGF. Interestingly, we confirmed that retina only expressed the isoform of PDGFA that lacks the cell retention motif, and this short PDGFA isoform was equally efficient in attracting astrocytes as the matrix-bound long PDGFA isoform. This is in contrast with vascular endothelial growth factor A (VEGFA), which requires interaction with HSPGs in the ECM to form a gradient to regulate angiogenesis (Ruhrberg et al., 2002; Stalmans et al., 2002). Without a cell-retention motif to bind to proteoglycans on the retinal surface, how does PDGFA maintain a chemoattractive gradient to provide directional cues for astrocyte migration? We would like to speculate that astrocytes may actively internalize and degrade extracellular PDGFA as they spread across the retina, depleting PDGFA in the wake of their migration wave. This leaves free PDGFA available only in front of astrocytes, resulting in a self-generated gradient that propels astrocytes to invade the unpopulated retina.

The most intriguing finding of our study is that cell-surface HS and CS are required for basement membrane assembly. Although there is in vitro evidence that HS and CS can bind laminins (Bachy et al., 2008; Elias et al., 1999; Ogawa et al., 2007), it was previously reported that the removal of HS or CS from the surface of Schwann cells by heparinase or ChABC treatment respectively failed to block laminin polymerization (Li et al., 2002). Instead, sulfated glycolipids, which bind the same residues on the laminin LG module as HS, were found to be both necessary and sufficient for laminin accumulation on the cell surface (Li et al., 2005). Based on these results, it is currently thought that sulfated glycolipids and not GAGs are the genuine cellular receptors for basement membrane assembly (Yurchenco, 2015). Nevertheless, it is previously reported that expression of truncated syndecan-2 proteoglycan lacking the cytoplasmic domain interfered with the assembly of laminin and fibronectin into a fibrillar matrix in Chinese hamster ovary (CHO) cells, even though this was thought to be caused by defective PKA signaling and not the lack of GAG chains (Klass et al., 2000). On the other hand, the myofiber basal laminae in syndecan-4 knockout mice was found to be disorganized and reduced in thickness (Cornelison et al., 2004). By genetically blocking the biosynthetic pathway for all GAGs, we now show that the loss of retinal-derived proteoglycans leads to disruption of the retinal basement membrane. It is important to note that our retinal-specific ablation of GAGs does not affect secreted proteoglycans such as perlecan and collagen XVIII residing in the ILM, because they are produced by the lens and ciliary body, not by the retina (Dong et al., 2003; Halfter et al., 2000). Instead, results from our ILM assembly assay showed that removal of the membrane-bound HS and CS interfered with the ability of the retina to assemble the ILM. The redundancy of HS and CS is further supported by the phenotypic disparity between GAG and HS mutants, which demonstrated that the loss of HS alone was not sufficient to disrupt the ILM formation. Our study suggests that the role of CS and HS in basement membrane formation may have been obscured by their functional redundancy. Moreover, we propose that proteoglycans belong to the repertoire of cellular receptors including integrins, dystroglycan and sulfated glycolipids that are capable of interacting with extracellular laminins. Interfering with any one of the cellular receptors will likely have limited impact, depending on the tissue-specific expression levels of these factors. This explains the lack of universal basement membrane defects in HS, CS, integrin, and dystroglycan mutants. How these cellular receptors cooperate to interact with the laminins may be the key to determine the tissue-specific competence for the basement membrane assembly.

The breach of the ILM is a common feature of diabetic retinopathy and proliferative vitreoretinopathy (Varshney et al., 2015). In addition, our study shows that retinal specific ablation of proteoglycans also results in hyaloid vessel persistence, a hallmark of ROP and familial exudative vitreoretinopathy (FEVR). The failure of hyaloid vessel regression has been observed in mouse mutants lacking basement membrane proteins including laminin α1, β2, γ3, and collagen XVIII, suggesting that defective ILM is likely the underlying cause of abnormal hyaloid vessels (Edwards

et al., 2010; Fukai et al., 2002; Gnanaguru et al., 2013). In these animals, astrocytes were frequently found to migrate into the vitreous, clinging to the remaining hyaloid vessels, a phenotype also observed in our proteoglycan mutants. We propose that the ILM serves both as a migratory substratum for astrocytes and a physical barrier to prevent astrocytes from straying into the vitreous and the hyaloid vessels from invading the retina. The failure of retinal angiogenesis as a result of astrocyte migration defects also induces an upregulation of VEGF in the deep layer of the retina, as observed in our proteoglycan mutant, which further promotes the invasion and survival of hyaloid vessels in the neural retina. Although we are unable to test this hypothesis directly by restoring the ILM in our proteoglycan mutant, the coincidence of finding a defective ILM and abnormal astrocytes and hyaloid vessels is consistent with this model. In human, persistent fetal vasculature is one of the key ocular defects in Pierson syndrome caused by *LAMB2* mutations and in Knobloch syndrome by *Collagen XVIII* mutations, and both may progress to retinal detachment and blindness (Duh et al., 2004; Mohney et al., 2011). By revealing a role of retinal-derived proteoglycans in ILM assembly, our study suggests that retinal proteoglycans may be important factors in understanding the pathology of these blinding diseases.

EXPERIMENTAL PROCEDURES

Mice

Ugdh^{flox} mice have been previously reported (Qu et al., 2012). *α-Cre* and *Six3-Cre* mice were kindly provided by Drs. Ruth Ashery-Padan (Tel Aviv University, Tel Aviv, Israel) and Yasuhide Furuta (M.D. Anderson Cancer Center, Houston, TX), respectively (Furuta et al., 2000; Marquardt et al., 2001). *LSL-Kras*^{G12D} mice were obtained from the Mouse Models of Human Cancers Consortium (MMHCC) Repository at the National Cancer Institute (Tuveson et al., 2004). *PDGFRα*^{flox} (stock number 006492), *PDGFRα*^{GFP} (stock number 007669), and *GFAP-Cre* (stock number 004600) mice were from Jackson Laboratory (Hamilton et al., 2003; Tallquist and Soriano, 2003; Zhuo et al., 2001). *Ext1*^{flox} (stock number 011699-UCD) mice were from Mutant Mouse Resource Research Centers (MMRRC). All mice were maintained in mixed genetic background, and experiments were performed in accordance with institutional guidelines. The animal experiments were approved by Columbia University Institutional Animal Care and Use Committee (IACUC).

Immunohistochemistry and RNA In Situ Hybridization

Whole retina fixed in 4% PFA or 10 μm rehydrated cryosections were blocked with 10% normal goat serum (NGS) for 1 hr at room temperature and incubated with first antibody overnight at 4°C (Cai et al., 2011). After washing with PBS, samples were incubated with second fluorescent-conjugated antibody in 2% BSA for 1 hr at room temperature in dark. Isolectin GS-IB$_4$ (IB4) conjugated with Alexa 488 (#I21411, Thermo Fisher Scientific) was applied to visualize the vasculature. Samples were washed and mounted with n-propyl gallate (NPG) anti-fading reagent and examined under a Leica DM5000-B fluorescent microscope. Antibodies used were anti-BrdU (G3G4, Developmental Studies Hybridoma Bank [DSHB]), anti-Brn3a (#MAB1585, Chemicon), anti-β3-tubulin (#5568, Cell Signaling Technology), anti-Chx10 (X1179P, Exalpha), anti-Col IV (#AB756P, EMD Millipore), anti-GFAP (#Z0334, Dako), anti-Ki-67(#550609, BD Pharmingen), anti-laminin (#L9393, Sigma-Aldrich), anti-NF165 (2H3, DSHB), anti-pax2 (#RB-276P, Covance), anti-pax6 (#PRB-278P, Covance), Alexa 488 Phalloidin (#A12379, Life Technologies), anti-rhodopsin (O4886, Sigma-Aldrich), and anti-Sox2 (sc-17320, Santa Cruz Biotechnology). Anti-perlecan antibody was a kind gift from Dr. Peter Yurchenco (Rutgers University, Piscataway, NJ).

RNA in situ hybridization was performed as previously described (Carbe et al., 2012; Carbe and Zhang, 2011). *VEGFA* probe was a kind gift from Dr. Marcus Fruttiger (University College London, London, UK). *Perlecan* probe was generated from a full-length cDNA clone (IMAGE: 3497930).

qRT-PCR

Total RNAs were extracted from postnatal day 3 retinal or kidney samples using TRIZOL (#15596, Life Technologies), as instructed by the product manual, and converted to cDNA using the SuperScript III Reverse Transcriptase kit (#18080, Invitrogen) (Carbe et al., 2013). Two sets of primers were designed to detect the isoform-specific expression of *PDGFA*. The first set targets exon 6 which is absent from *PDGFA* short isoform due to alternative splicing (sense: 5′-GCGGAAAAGGAAAAGGTTAAAAC-3′; antisense: 5′-GGCTCATCT CACCTCACATCTG-3′); the second set spans exons 4 and 5, which are present in both long and short isoforms (sense: 5′-GGTCCACCACCGCA GTGT-3′; antisense: 5′-CAATTTTGGCTTCTTCCTGACAT-3′). qRT-PCR was performed with the SYBR Green PCR Master Mix (4367659, Applied Biosystems) and analyzed on a StepOnePlus Real-Time PCR instrument (Applied Biosystems). Relative standard curves were generated by serial dilutions, and all samples were run in triplicate.

Ligand and Carbohydrate Engagement Assays

HSPGs was detected by LACE assay as previously described (Allen and Rapraeger, 2003; Pan et al., 2006). Briefly, enucleated eyeballs were fixed in 4% PFA overnight at 4°C prior to paraffin embedding. 10-μm sections were deparaffinized and rehydrated, followed by incubation in 0.5 mg/mL $NaBH_4$ for 10 min, 0.1M glycine for 30 min and PBS washing for 3 times. After blocking with 2% BSA for 1 hr at room temperature, sections were incubated with 20 μM recombinant human FGF-10 (#345-FG, R&D Systems) and 20 μM human FGFR2α (IIIb)/Fc chimera (#663-FR, R&D systems) in DMEM (#10-013-CV, Corning Life Sciences) with 10% fetal bovine serum (FBS) at 4°C overnight. Cy3-labeled anti-human Fc second antibody was applied the next day after PBS washing. The slides may be further processed for regular immunohistochemistry and mounted with NPG reagent for examination. For LACE assay on whole-mount retina, retinae were fixed in 4% PFA for 1 hr at 4°C, washed with PBS, and blocked by 2% BSA, followed by incubation with FGF-fibroblast growth factor receptor (FGFR) mixture overnight and visualized by cy3-labeled anti-human Fc second antibody as described above.

Ex Vivo Astrocyte Migration Assay

P0 retinae were dissected in DMEM, quartered to petals, and flat mounted onto 0.45-μm membrane filters (#HAWP01300, EMD Millipore) with the vitreal side facing up. Affi-Gel Blue Gel agarose beads (#1537302, Bio-Rad) pre-incubated with 100 μg/mL PDGFA$_L$ (#221-AA, R&D Systems) or PDGFA$_S$ (#1055-AA, R&D Systems) were carefully placed on the periphery of the retinal using forceps. Beads pre-incubated with 2% BSA were included as controls. The liquid-air interface was maintained by floating the membrane filters on DMEM supplemented with 10% FBS and cultured at 37°C with 5% CO_2. After 2 days, the retinal whole mounts were fixed with 4% PFA for 1 hr and processed for immunohistochemistry as described above. For time-lapse imaging, flat-mounted retina was placed on a 24-mm transwell insert (#3450, Corning Life Sciences) with the vitreal side facing up. Pre-coated beads were placed at the peripheral retina as described above. The insert was placed on a 35-mm glass-bottomed imaging dish (#81156, ibidi) filled with DMEM-10% FBS and cultured in a stage top incubator chamber with environmental control unit (IV-ECU-HC, In Vivo Scientific) to maintain the temperature at 37°C and the CO_2 level at 5%. The culture was imaged with an inverted fluorescent microscope (ECLIPSE Ti, Nikon) with a Perfect Focus System (PFS) at an interval of 7 min for 2 days.

Matrigel Reconstitution Assay

P0 retinae were dissected out and digested with 20 U/mL collagenase from *Clostridium histolyticum* (#C0773, Sigma-Aldrich) alone or in combination with 1 U/mL heparinase I and III Blend from *Flavobacterium heparinum* (#H3917, Sigma-Aldrich) and/or 1 U/mL chondroitinase ABC from *Proteus vulgaris* (ChABC; #C2905, Sigma-Aldrich) in DMEM for 20 hr at 37°C with 5% CO_2. Digestion was stopped by transferring retinae to DMEM with 10% FBS. Retinae were quartered and flat mounted onto a membrane filter with the vitreal side up. 10 μL Matrigel Matrix (#356234, Corning Life Sciences) supplemented with 100 μg/mL laminin (#CB-40232, Thermo Fisher Scientific) was added on top of each retinal

whole mount. After the Matrigel solidified, membrane filters were floated on DMEM/10% FBS and incubated at 37°C with 5% CO_2 for 2 days. After incubation, the culture was washed in ice-cold PBS for 30 min to remove the Matrigel and fixed with 4% PFA at 4°C for 1 hr. Immunohistochemistry on whole-mount retinae was conducted as described above. The percentage of ILM reconstitution was quantified by NIS-Elements AR Software (Nikon) as the ratio of laminin-positive area versus the total area of retinal whole mount imaged. At least three images were taken from different regions of one retina. Data from different digestion groups were compared using one-way ANOVA.

SUPPLEMENTAL INFORMATION

Supplemental Information includes three figures and can be found with this article online at http://dx.doi.org/10.1016/j.celrep.2016.10.035.

AUTHOR CONTRIBUTIONS

C.T. conducted the experiment. C.T. and X.Z. designed the experiments and wrote the paper.

ACKNOWLEDGMENTS

The authors thank Drs. Marcus Fruttiger and Peter Yurchenco for reagents, Frank Costantini and Richard Vallee for help with time-lapse imaging and Frank Costantini and Carol Mason for critical reading of the manuscript. This work was supported by NIH grants EY017061, EY018868, and EY025933 (X.Z.). The Columbia Ophthalmology Core Facility is supported by NIH core grant 5P30EY019007 and unrestricted funds from Research to Prevent Blindness. X.Z. is supported by Jules and Doris Stein Research to Prevent Blindness Professorship.

Received: May 27, 2016
Revised: September 16, 2016
Accepted: October 12, 2016
Published: November 8, 2016

REFERENCES

Abramsson, A., Kurup, S., Busse, M., Yamada, S., Lindblom, P., Schallmeiner, E., Stenzel, D., Sauvaget, D., Ledin, J., Ringvall, M., et al. (2007). Defective N-sulfation of heparan sulfate proteoglycans limits PDGF-BB binding and pericyte recruitment in vascular development. Genes Dev. *21*, 316–331.

Allen, B.L., and Rapraeger, A.C. (2003). Spatial and temporal expression of heparan sulfate in mouse development regulates FGF and FGF receptor assembly. J. Cell Biol. *163*, 637–648.

Bachy, S., Letourneur, F., and Rousselle, P. (2008). Syndecan-1 interaction with the LG4/5 domain in laminin-332 is essential for keratinocyte migration. J. Cell. Physiol. *214*, 238–249.

Bishop, J.R., Schuksz, M., and Esko, J.D. (2007). Heparan sulphate proteoglycans fine-tune mammalian physiology. Nature *446*, 1030–1037.

Cai, Z., Simons, D.L., Fu, X.Y., Feng, G.S., Wu, S.M., and Zhang, X. (2011). Loss of Shp2-mediated mitogen-activated protein kinase signaling in Muller glial cells results in retinal degeneration. Mol. Cell. Biol. *31*, 2973–2983.

Cai, Z., Tao, C., Li, H., Ladher, R., Gotoh, N., Feng, G.S., Wang, F., and Zhang, X. (2013). Deficient FGF signaling causes optic nerve dysgenesis and ocular coloboma. Development *140*, 2711–2723.

Cai, Z., Grobe, K., and Zhang, X. (2014). Role of heparan sulfate proteoglycans in optic disc and stalk morphogenesis. Dev. Dyn. *243*, 1310–1316.

Carbe, C., and Zhang, X. (2011). Lens induction requires attenuation of ERK signaling by Nf1. Hum. Mol. Genet. *20*, 1315–1323.

Carbe, C., Hertzler-Schaefer, K., and Zhang, X. (2012). The functional role of the Meis/Prep-binding elements in Pax6 locus during pancreas and eye development. Dev. Biol. *363*, 320–329.

Carbe, C., Garg, A., Cai, Z., Li, H., Powers, A., and Zhang, X. (2013). An allelic series at the paired box gene 6 (Pax6) locus reveals the functional specificity of Pax genes. J. Biol. Chem. *288*, 12130–12141.

Chu, Y., Hughes, S., and Chan-Ling, T. (2001). Differentiation and migration of astrocyte precursor cells and astrocytes in human fetal retina: relevance to optic nerve coloboma. FASEB J. *15*, 2013–2015.

Cornelison, D.D., Wilcox-Adelman, S.A., Goetinck, P.F., Rauvala, H., Rapraeger, A.C., and Olwin, B.B. (2004). Essential and separable roles for Syndecan-3 and Syndecan-4 in skeletal muscle development and regeneration. Genes Dev. *18*, 2231–2236.

Costell, M., Gustafsson, E., Aszódi, A., Mörgelin, M., Bloch, W., Hunziker, E., Addicks, K., Timpl, R., and Fässler, R. (1999). Perlecan maintains the integrity of cartilage and some basement membranes. J. Cell Biol. *147*, 1109–1122.

Dong, S., Cole, G.J., and Halfter, W. (2003). Expression of collagen XVIII and localization of its glycosaminoglycan attachment sites. J. Biol. Chem. *278*, 1700–1707.

Dorrell, M.I., and Friedlander, M. (2006). Mechanisms of endothelial cell guidance and vascular patterning in the developing mouse retina. Prog. Retin. Eye Res. *25*, 277–295.

Duan, L.J., Takeda, K., and Fong, G.H. (2014). Hypoxia inducible factor-2 alpha regulates the development of retinal astrocytic network by maintaining adequate supply of astrocyte progenitors. PLoS ONE *9*, e84736.

Duh, E.J., Yao, Y.G., Dagli, M., and Goldberg, M.F. (2004). Persistence of fetal vasculature in a patient with Knobloch syndrome: potential role for endostatin in fetal vascular remodeling of the eye. Ophthalmology *111*, 1885–1888.

Edwards, M.M., Mammadova-Bach, E., Alpy, F., Klein, A., Hicks, W.L., Roux, M., Simon-Assmann, P., Smith, R.S., Orend, G., Wu, J., et al. (2010). Mutations in Lama1 disrupt retinal vascular development and inner limiting membrane formation. J. Biol. Chem. *285*, 7697–7711.

Edwards, M.M., McLeod, D.S., Li, R., Grebe, R., Bhutto, I., Mu, X., and Lutty, G.A. (2012). The deletion of Math5 disrupts retinal blood vessel and glial development in mice. Exp. Eye Res. *96*, 147–156.

Elias, M.C., Veiga, S.S., Gremski, W., Porcionatto, M.A., Nader, H.B., and Brentani, R.R. (1999). Presence of a laminin-binding chondroitin sulfate proteoglycan at the cell surface of a human melanoma cell Mel-85. Mol. Cell. Biochem. *197*, 39–48.

Esko, J.D., and Selleck, S.B. (2002). Order out of chaos: assembly of ligand binding sites in heparan sulfate. Annu. Rev. Biochem. *71*, 435–471.

Feyzi, E., Lustig, F., Fager, G., Spillmann, D., Lindahl, U., and Salmivirta, M. (1997). Characterization of heparin and heparan sulfate domains binding to the long splice variant of platelet-derived growth factor A chain. J. Biol. Chem. *272*, 5518–5524.

Forsberg-Nilsson, K., Behar, T.N., Afrakhte, M., Barker, J.L., and McKay, R.D.G. (1998). Platelet-derived growth factor induces chemotaxis of neuroepithelial stem cells. J. Neurosci. Res. *53*, 521–530.

Fruttiger, M., Calver, A.R., Krüger, W.H., Mudhar, H.S., Michalovich, D., Takakura, N., Nishikawa, S., and Richardson, W.D. (1996). PDGF mediates a neuron-astrocyte interaction in the developing retina. Neuron *17*, 1117–1131.

Fukai, N., Eklund, L., Marneros, A.G., Oh, S.P., Keene, D.R., Tamarkin, L., Niemelä, M., Ilves, M., Li, E., Pihlajaniemi, T., and Olsen, B.R. (2002). Lack of collagen XVIII/endostatin results in eye abnormalities. EMBO J. *21*, 1535–1544.

Furuta, Y., Lagutin, O., Hogan, B.L., and Oliver, G.C. (2000). Retina- and ventral forebrain-specific Cre recombinase activity in transgenic mice. Genesis *26*, 130–132.

Gerhardt, H., Golding, M., Fruttiger, M., Ruhrberg, C., Lundkvist, A., Abramsson, A., Jeltsch, M., Mitchell, C., Alitalo, K., Shima, D., and Betsholtz, C. (2003). VEGF guides angiogenic sprouting utilizing endothelial tip cell filopodia. J. Cell Biol. *161*, 1163–1177.

Gnanaguru, G., Bachay, G., Biswas, S., Pinzón-Duarte, G., Hunter, D.D., and Brunken, W.J. (2013). Laminins containing the β2 and γ3 chains regulate astrocyte migration and angiogenesis in the retina. Development *140*, 2050–2060.

Häcker, U., Nybakken, K., and Perrimon, N. (2005). Heparan sulphate proteoglycans: the sweet side of development. Nat. Rev. Mol. Cell Biol. *6*, 530–541.

Halfter, W., Dong, S., Schurer, B., Osanger, A., Schneider, W., Ruegg, M., and Cole, G.J. (2000). Composition, synthesis, and assembly of the embryonic chick retinal basal lamina. Dev. Biol. *220*, 111–128.

Halfter, W., Dong, S., Schurer, B., Ring, C., Cole, G.J., and Eller, A. (2005). Embryonic synthesis of the inner limiting membrane and vitreous body. Invest. Ophthalmol. Vis. Sci. *46*, 2202–2209.

Halfter, W., Dong, S., Dong, A., Eller, A.W., and Nischt, R. (2008). Origin and turnover of ECM proteins from the inner limiting membrane and vitreous body. Eye (Lond.) *22*, 1207–1213.

Hamilton, T.G., Klinghoffer, R.A., Corrin, P.D., and Soriano, P. (2003). Evolutionary divergence of platelet-derived growth factor alpha receptor signaling mechanisms. Mol. Cell. Biol. *23*, 4013–4025.

Hirota, S., Liu, Q., Lee, H.S., Hossain, M.G., Lacy-Hulbert, A., and McCarty, J.H. (2011). The astrocyte-expressed integrin αvβ8 governs blood vessel sprouting in the developing retina. Development *138*, 5157–5166.

Hohenester, E., and Yurchenco, P.D. (2013). Laminins in basement membrane assembly. Cell Adhes. Migr. *7*, 56–63.

Kang, J., Gu, Y., Li, P., Johnson, B.L., Sucov, H.M., and Thomas, P.S. (2008). PDGF-A as an epicardial mitogen during heart development. Dev. Dyn. *237*, 692–701.

Klass, C.M., Couchman, J.R., and Woods, A. (2000). Control of extracellular matrix assembly by syndecan-2 proteoglycan. J. Cell Sci. *113*, 493–506.

Lang, R.A. (1997). Apoptosis in mammalian eye development: lens morphogenesis, vascular regression and immune privilege. Cell Death Differ. *4*, 12–20.

Li, S., Harrison, D., Carbonetto, S., Fassler, R., Smyth, N., Edgar, D., and Yurchenco, P.D. (2002). Matrix assembly, regulation, and survival functions of laminin and its receptors in embryonic stem cell differentiation. J. Cell Biol. *157*, 1279–1290.

Li, S., Liquari, P., McKee, K.K., Harrison, D., Patel, R., Lee, S., and Yurchenco, P.D. (2005). Laminin-sulfatide binding initiates basement membrane assembly and enables receptor signaling in Schwann cells and fibroblasts. J. Cell Biol. *169*, 179–189.

Marquardt, T., Ashery-Padan, R., Andrejewski, N., Scardigli, R., Guillemot, F., and Gruss, P. (2001). Pax6 is required for the multipotent state of retinal progenitor cells. Cell *105*, 43–55.

Mohney, B.G., Pulido, J.S., Lindor, N.M., Hogan, M.C., Consugar, M.B., Peters, J., Pankratz, V.S., Nasr, S.H., Smith, S.J., Gloor, J., et al. (2011). A novel mutation of LAMB2 in a multigenerational mennonite family reveals a new phenotypic variant of Pierson syndrome. Ophthalmology *118*, 1137–1144.

Morgan, J.E. (2000). Optic nerve head structure in glaucoma: astrocytes as mediators of axonal damage. Eye (Lond.) *14* (*Pt 3B*), 437–444.

Ogawa, T., Tsubota, Y., Hashimoto, J., Kariya, Y., and Miyazaki, K. (2007). The short arm of laminin gamma2 chain of laminin-5 (laminin-332) binds syndecan-1 and regulates cellular adhesion and migration by suppressing phosphorylation of integrin beta4 chain. Mol. Biol. Cell *18*, 1621–1633.

Pan, Y., Woodbury, A., Esko, J.D., Grobe, K., and Zhang, X. (2006). Heparan sulfate biosynthetic gene Ndst1 is required for FGF signaling in early lens development. Development *133*, 4933–4944.

Pan, Y., Carbe, C., Powers, A., Zhang, E.E., Esko, J.D., Grobe, K., Feng, G.S., and Zhang, X. (2008). Bud specific N-sulfation of heparan sulfate regulates Shp2-dependent FGF signaling during lacrimal gland induction. Development *135*, 301–310.

Pinzón-Duarte, G., Daly, G., Li, Y.N., Koch, M., and Brunken, W.J. (2010). Defective formation of the inner limiting membrane in laminin beta2- and gamma3-null mice produces retinal dysplasia. Invest. Ophthalmol. Vis. Sci. *51*, 1773–1782.

Qu, X., Pan, Y., Carbe, C., Powers, A., Grobe, K., and Zhang, X. (2012). Glycosaminoglycan-dependent restriction of FGF diffusion is necessary for lacrimal gland development. Development *139*, 2730–2739.

Rolny, C., Spillmann, D., Lindahl, U., and Claesson-Welsh, L. (2002). Heparin amplifies platelet-derived growth factor (PDGF)- BB-induced PDGF alpha -receptor but not PDGF beta -receptor tyrosine phosphorylation in heparan sulfate-deficient cells. Effects on signal transduction and biological responses. J. Biol. Chem. *277*, 19315–19321.

Ruhrberg, C., Gerhardt, H., Golding, M., Watson, R., Ioannidou, S., Fujisawa, H., Betsholtz, C., and Shima, D.T. (2002). Spatially restricted patterning cues provided by heparin-binding VEGF-A control blood vessel branching morphogenesis. Genes Dev. *16*, 2684–2698.

Sapieha, P., Sirinyan, M., Hamel, D., Zaniolo, K., Joyal, J.S., Cho, J.H., Honoré, J.C., Kermorvant-Duchemin, E., Varma, D.R., Tremblay, S., et al. (2008). The succinate receptor GPR91 in neurons has a major role in retinal angiogenesis. Nat. Med. *14*, 1067–1076.

Schnitzer, J. (1987). Retinal astrocytes: their restriction to vascularized parts of the mammalian retina. Neurosci. Lett. *78*, 29–34.

Scott, A., and Fruttiger, M. (2010). Oxygen-induced retinopathy: a model for vascular pathology in the retina. Eye (Lond.) *24*, 416–421.

Scott, A., Powner, M.B., Gandhi, P., Clarkin, C., Gutmann, D.H., Johnson, R.S., Ferrara, N., and Fruttiger, M. (2010). Astrocyte-derived vascular endothelial growth factor stabilizes vessels in the developing retinal vasculature. PLoS ONE *5*, e11863.

Smith, E.M., Mitsi, M., Nugent, M.A., and Symes, K. (2009). PDGF-A interactions with fibronectin reveal a critical role for heparan sulfate in directed cell migration during Xenopus gastrulation. Proc. Natl. Acad. Sci. USA *106*, 21683–21688.

Stalmans, I., Ng, Y.S., Rohan, R., Fruttiger, M., Bouché, A., Yuce, A., Fujisawa, H., Hermans, B., Shani, M., Jansen, S., et al. (2002). Arteriolar and venular patterning in retinas of mice selectively expressing VEGF isoforms. J. Clin. Invest. *109*, 327–336.

Stenzel, D., Lundkvist, A., Sauvaget, D., Busse, M., Graupera, M., van der Flier, A., Wijelath, E.S., Murray, J., Sobel, M., Costell, M., et al. (2011). Integrin-dependent and -independent functions of astrocytic fibronectin in retinal angiogenesis. Development *138*, 4451–4463.

Stone, J., and Dreher, Z. (1987). Relationship between astrocytes, ganglion cells and vasculature of the retina. J. Comp. Neurol. *255*, 35–49.

Stone, J., Chan-Ling, T., Pe'er, J., Itin, A., Gnessin, H., and Keshet, E. (1996). Roles of vascular endothelial growth factor and astrocyte degeneration in the genesis of retinopathy of prematurity. Invest. Ophthalmol. Vis. Sci. *37*, 290–299.

Tallquist, M.D., and Soriano, P. (2003). Cell autonomous requirement for PDGFRalpha in populations of cranial and cardiac neural crest cells. Development *130*, 507–518.

Tao, C., and Zhang, X. (2014). Development of astrocytes in the vertebrate eye. Dev. Dyn. *243*, 1501–1510.

Tuveson, D.A., Shaw, A.T., Willis, N.A., Silver, D.P., Jackson, E.L., Chang, S., Mercer, K.L., Grochow, R., Hock, H., Crowley, D., et al. (2004). Endogenous oncogenic K-ras(G12D) stimulates proliferation and widespread neoplastic and developmental defects. Cancer Cell *5*, 375–387.

Uemura, A., Kusuhara, S., Wiegand, S.J., Yu, R.T., and Nishikawa, S. (2006). Tlx acts as a proangiogenic switch by regulating extracellular assembly of fibronectin matrices in retinal astrocytes. J. Clin. Invest. *116*, 369–377.

Varshney, S., Hunter, D.D., and Brunken, W.J. (2015). Extracellular matrix components regulate cellular polarity and tissue structure in the developing and mature retina. J. Ophthalmic Vis. Res. *10*, 329–339.

Volterra, A., and Meldolesi, J. (2005). Astrocytes, from brain glue to communication elements: the revolution continues. Nat. Rev. Neurosci. *6*, 626–640.

Weidemann, A., Krohne, T.U., Aguilar, E., Kurihara, T., Takeda, N., Dorrell, M.I., Simon, M.C., Haase, V.H., Friedlander, M., and Johnson, R.S. (2010). Astrocyte hypoxic response is essential for pathological but not developmental angiogenesis of the retina. Glia *58*, 1177–1185.

Yurchenco, P.D. (2015). Integrating activities of laminins that drive basement membrane assembly and function. Curr. Top. Membr. *76*, 1–30.

Yurchenco, P.D., and Patton, B.L. (2009). Developmental and pathogenic mechanisms of basement membrane assembly. Curr. Pharm. Des. *15*, 1277–1294.

Zhuo, L., Theis, M., Alvarez-Maya, I., Brenner, M., Willecke, K., and Messing, A. (2001). hGFAP-cre transgenic mice for manipulation of glial and neuronal function in vivo. Genesis *31*, 85–94.